Energy exhanges in a system of a forced linear structure coupled to a chain of nonlinear oscillators

Simon Charlemagne*, Alireza Ture Savadkoohi* and Claude-Henri Lamarque*
*Univ Lyon, ENTPE, LTDS UMR CNRS 5513, Rue Maurice Audin, F-69518, Vaulx-en-Velin Cedex, France

Summary. A system consisting of a forced main linear structure coupled to a chain of nonlinear oscillators is studied. Time multi-scales dynamics of the set reveals the existence of a Slow Invariant Manifold (SIM) at fast time scale, housing all possible asymptotic states of the system. At slow time scale, equilibrium and singular points, hints of periodic regimes and Strongly Modulated Responses (SMR), are detected. During periodic regimes, energy is localized in the chain in the form of nonlinear modes, whereas SMR is characterized by persistent bifurcations between several modes of the chain. Finally, numerical simulations are compared to analytical predictions, showing a good agreement.

Introduction

Nonlinear devices are known for being efficient at passively controlling a master structure [1]. One of them is the Nonlinear Energy Sink (NES) [2–4] whose essential nonlinearity enables to capture resonance of the main system for a wide frequency range. Recent advances have shown the efficiency of two or three nonlinear oscillators in series [5–7].
Here, we extend this idea to the study of an arbitrary number of nonlinear oscillators in series coupled to a linear system. Similar chains have been studied by Starosvetsky and Vakakis [8] who place a granular media between two rods for purposes of shock mitigation. Properties of passive attenuation of propagating pulses and vibration isolation were also found in dimer chains and two-dimensional granular network by Jayaprakash et al. [9] and Hasan et al. [10] respectively. The analytical method used in this paper aims to give tools to design finite chains to perform passive control of structures. However, the present work differs from the aforementioned references as we intend to study the energy transfer to the chain from a main system submitted to harmonic solicitation and oscillating at a single frequency. The model and the method are first explained, then numerical simulations confirm analytical predictions.

Presentation of the model

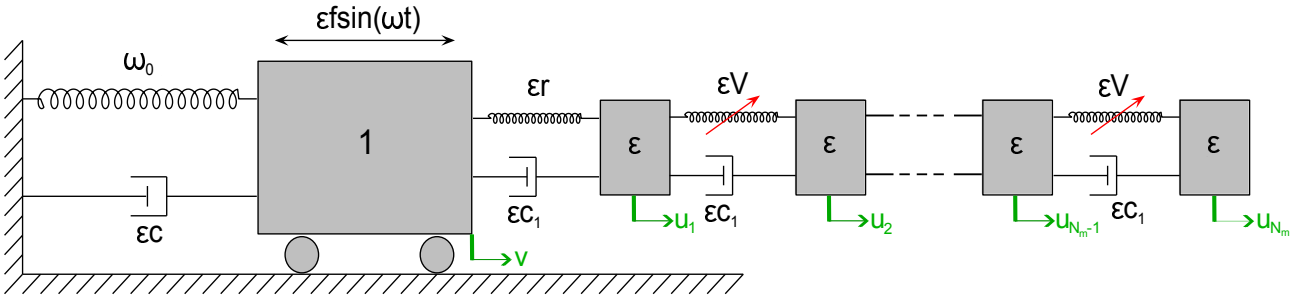

Figure 1: $(N+1)$ degree-of-freedom model consisting of a linear structure coupled to a chain of N_m nonlinear oscillators $(0 < \epsilon \ll 1)$

We consider a single-degree-of-freedom (dof) linear structure, with the natural frequency and damping ω_0 and ϵc, coupled to N_m nonlinear oscillators of mass $\epsilon \ll 1$ in series (see Fig. 1). The main system is linearly attached to the chain through a spring of stiffness ϵr and a damping ϵc_1. Connection between each mass of the chain is provided by a nonlinear restoring force $\epsilon V(z) = \epsilon(Bz + Dz^3)$ and a damping ϵc_1. The linear system is subjected to external harmonic forcing $\epsilon f^0 \sin(\omega t)$. Furthermore, we aim to investigate the dynamics of the system around resonance of the main structure, so we assume that ω is close to ω_0, i.e. $\omega^2 = \omega_0^2(1 + \sigma\epsilon)$ where σ is a detuning parameter. Thus, governing equations of the system read:

$$\begin{cases} \ddot{v} + \epsilon c\dot{v} + \omega_0^2 v + \epsilon c_1(\dot{v} - \dot{u}_1) + \epsilon r(v - u_1) = \epsilon f \sin(\omega t) \\ \ddot{u}_1 + c_1(-\dot{v} + 2\dot{u}_1 - \dot{u}_2) + r(u_1 - v) + B(u_1 - u_2) + D(u_1 - u_2)^3 = 0 \\ \ddot{u}_2 + c_1(-\dot{u}_1 + 2\dot{u}_2 - \dot{u}_1) + B(-u_1 + 2u_2 - u_3) + D(u_2 - u_1)^3 + D(u_2 - u_3)^3 = 0 \\ \qquad\qquad \vdots \\ \ddot{u}_j + c_1(-\dot{u}_{j-1} + 2\dot{u}_j - \dot{u}_{j+1}) + B(-u_{j-1} + 2u_j - u_{j+1}) + D(u_j - u_{j-1})^3 + D(u_j - u_{j+1})^3 = 0 \\ j = 3, \ldots, N_m - 1 \\ \qquad\qquad \vdots \\ \ddot{u}_{N_m} + c_1(\dot{u}_{N_m} - \dot{u}_{N_m-1}) + B(u_{N_m} - u_{N_m-1}) + D(u_{N_m} - u_{N_m-1})^3 = 0 \end{cases} \tag{1}$$

where v denotes the displacement of the main structure and u_j, $j = 1 \ldots N_m$ the displacements of the nonlinear oscillators.

Analytical methodology

Treatment of Eqs. (1) generalizes the methodology described in [11] and mobilizes different tools.

- We introduce complex variables of Manevitch [12] ψ and φ_j, $j = 1, \ldots, N_m$ ($i = \sqrt{-1}$):

$$\left\{ \begin{array}{l} \psi e^{i\omega t} = \dot{v} + i\omega v \\ \varphi_j e^{i\omega t} = \dot{w}_j + i\omega w_j \end{array} \right. \quad \text{where} \quad \left\{ \begin{array}{l} w_1 = u_1 - v \\ w_l = u_l - u_{l-1}, \quad l = 2, \ldots, N_m \end{array} \right. \tag{2}$$

  Those variables describe slow modulation of fast oscillating variables v and w_j, i.e. oscillating at the frequency ω.

- A multiple scale method [13] is implemented by embedding time at different time scales $\tau_k = \epsilon^k t$, $k = 0, 1, 2, \ldots$, where τ_0 is the fast time scale and τ_k, $k = 1, 2, \ldots$ are slow time scales. We will analyze the system behaviors at those different time scales by deriving equations at the corresponding orders of ϵ.

- A Galerkin method enables to truncate high harmonics of the signal (i.e. frequencies $k\omega$, $k = 2, 3, \ldots$), which reads for an arbitrary function γ, assuming that γ does not depend on τ_0:

$$\Gamma = \frac{\omega}{2\pi} \int_0^{\frac{2\pi}{\omega}} \gamma(\tau_1, \tau_2, \ldots) e^{-i\omega\tau_0} d\tau_0 \tag{3}$$

  We will consider a priori that all complex variables ψ and φ_j do not depend on τ_0 (to be verified or constrained). We will also keep $\dot{\psi}$ and $\dot{\varphi}_j$ in the equations.

Analysis of system behaviors at fast and slow time scales

Deriving system equations at the ϵ^0 order, one obtains a system of the form:

$$\begin{pmatrix} \dfrac{\partial \psi}{\partial \tau_0} \\ \dfrac{\partial \varphi_1}{\partial \tau_0} \\ \vdots \\ \dfrac{\partial \varphi_{N_m}}{\partial \tau_0} \end{pmatrix} = \begin{pmatrix} 0 \\ \mathcal{S}_1 \\ \vdots \\ \mathcal{S}_{N_m} \end{pmatrix} \tag{4}$$

We are thus able to conclude that ψ does not depend on the fast time scale, i.e. $\dfrac{\partial \psi}{\partial \tau_0} = 0$. Furthermore, considering fix points ϕ_j ($j = 1, \ldots, N_m$) of the N_m remaining equations, i.e. those verifying $\lim\limits_{\tau_0 \to +\infty} \dfrac{\partial \phi_j}{\partial \tau_0} = 0$, we obtain the following system, namely the Slow Invariant Manifold (SIM):

$$\mathbf{M} \begin{pmatrix} \phi_1 \\ \phi_2 \\ \vdots \\ \phi_{N_m} \end{pmatrix} = -\frac{i\omega_0}{2} \begin{pmatrix} \psi \\ 0 \\ \vdots \\ 0 \end{pmatrix} \tag{5}$$

where

$$\mathbf{M} = \begin{pmatrix} \dfrac{i\omega_0}{2} + \alpha_1 & -\alpha + i\mathcal{D}N_2^2 & 0 & \cdots & 0 \\ -\alpha_1 & \dfrac{i\omega_0}{2} + 2\alpha - 2i\mathcal{D}N_2^2 & -\alpha + i\mathcal{D}N_3^2 & & \vdots \\ 0 & -\alpha + i\mathcal{D}N_2^2 & & & \vdots \\ \vdots & & \ddots & \ddots & 0 \\ \vdots & & & & -\alpha + i\mathcal{D}N_{N_m}^2 \\ 0 & \cdots & 0 & -\alpha + i\mathcal{D}N_{N_m-1}^2 & \dfrac{i\omega_0}{2} + 2\alpha - 2i\mathcal{D}N_{N_m}^2 \end{pmatrix} \tag{6}$$

$$\mathcal{D} = \frac{3D}{8\omega_0^3} \qquad \alpha = \frac{c_1}{2} - \frac{iB}{2\omega_0} \qquad \alpha_1 = \frac{c_1}{2} - \frac{ir}{2\omega_0}$$

$$\psi = Ne^{i\delta} \qquad \phi_j = N_j e^{i\delta_j} \quad j = 1, \ldots, N_m$$

The SIM gathers all possible asymptotic states of the system, whether they are stable or not.
Stability of the SIM is calculated by introducing an infinitesimal linear perturbation in system equations around the SIM as follows:

$$\begin{pmatrix} \varphi_2 \\ \vdots \\ \varphi_N \end{pmatrix} \rightarrow \begin{pmatrix} \phi_2 \\ \vdots \\ \phi_N \end{pmatrix} + \underbrace{\begin{pmatrix} \Delta\phi_2 \\ \vdots \\ \Delta\phi_N \end{pmatrix}}_{\Delta\Phi} \tag{7}$$

Injecting Eq. (7) into system (4), one obtains:

$$\begin{pmatrix} \dfrac{\partial \Delta\Phi}{\partial \tau_0} \\ \\ \dfrac{\partial \Delta\Phi^*}{\partial \tau_0} \end{pmatrix} = \mathbf{\Sigma} \begin{pmatrix} \Delta\Phi \\ \\ \Delta\Phi^* \end{pmatrix} \tag{8}$$

whre $.^*$ stands for the complex conjugate. Unstable zones are detected when the perturbation diverges versus time, i.e. when at least one eigenvalue of the matrix Σ presents a positive real part.
It is possible from system (5) to determine expressions of $(N-1)$ variables ϕ_j with respect to one remaining variable. Consequently, we need to examine the system at slow time scale τ_1 to obtain additional information and predict its final behavior.
Deriving the equation relative to the main system at the ϵ^1 order around the SIM leads to detection of:

- equilibrium points that describe the periodic regimes of the system during which variables ψ and ϕ_j tend to a constant value. It can be proven that above a certain level of energy, these periodic regimes take the form of nonlinear modes of the system. The excited mode depends on the level of energy transferred to the chain.
- singular points, which are hints of Strongly Modulated Responses (SMR) [14]. The SMR is characterized by persistent bifurcations between stable branches of the SIM, which here corresponds to bifurcations between modal behaviors.

Those points are detected as follows. Rewriting Eq. (5) under the form:

$$\mathcal{S} = \begin{pmatrix} \mathcal{S}_1 \\ \vdots \\ \mathcal{S}_{N_m} \end{pmatrix} = 0 \tag{9}$$

one can obtain the following matrix system:

$$\begin{cases} \dfrac{\partial \mathcal{S}_{j,r}}{\partial \tau_1} = 0 \\ \\ \dfrac{\partial \mathcal{S}_{j,i}}{\partial \tau_1} = 0 \end{cases} \qquad j = 1, \ldots, N_m$$

$$\Leftrightarrow \underbrace{\begin{pmatrix} \dfrac{\partial \mathcal{S}_{1,r}}{\partial N_1} & \cdots & \dfrac{\partial \mathcal{S}_{1,r}}{\partial N_{N_m}} & \dfrac{\partial \mathcal{S}_{1,r}}{\partial \delta_1} & \cdots & \dfrac{\partial \mathcal{S}_{1,r}}{\partial \delta_{N_m}} \\ \dfrac{\partial \mathcal{S}_{1,i}}{\partial N_1} & \cdots & \dfrac{\partial \mathcal{S}_{1,i}}{\partial N_{N_m}} & \dfrac{\partial \mathcal{S}_{1,i}}{\partial \delta_1} & \cdots & \dfrac{\partial \mathcal{S}_{1,i}}{\partial \delta_{N_m}} \\ \vdots & & \vdots & \vdots & & \vdots \\ \dfrac{\partial \mathcal{S}_{N_m,r}}{\partial N_1} & \cdots & \dfrac{\partial \mathcal{S}_{N_m,r}}{\partial N_{N_m}} & \dfrac{\partial \mathcal{S}_{N_m,r}}{\partial \delta_1} & \cdots & \dfrac{\partial \mathcal{S}_{N_m,r}}{\partial \delta_{N_m}} \\ \dfrac{\partial \mathcal{S}_{N_m,i}}{\partial N_1} & \cdots & \dfrac{\partial \mathcal{S}_{N_m,i}}{\partial N_{N_m}} & \dfrac{\partial \mathcal{S}_{N_m,i}}{\partial \delta_1} & \cdots & \dfrac{\partial \mathcal{S}_{N_m,i}}{\partial \delta_{N_m}} \end{pmatrix}}_{\mathbf{S}} \begin{pmatrix} \dfrac{\partial N_1}{\partial \tau_1} \\ \vdots \\ \dfrac{\partial N_{N_m}}{\partial \tau_1} \\ \dfrac{\partial \delta_1}{\partial \tau_1} \\ \vdots \\ \dfrac{\partial \delta_{N_m}}{\partial \tau_1} \end{pmatrix} = \frac{\omega_0}{2} \begin{pmatrix} \sin(\delta) & N\cos(\delta) \\ -\cos(\delta) & N\sin(\delta) \\ 0 & 0 \\ \vdots & \vdots \\ 0 & 0 \end{pmatrix} \begin{pmatrix} \dfrac{\partial N}{\partial \tau_1} \\ \\ \dfrac{\partial \delta}{\partial \tau_1} \end{pmatrix} \tag{10}$$

where $\mathcal{S}_{j,r}$ and $\mathcal{S}_{j,i}$ are real and imaginary parts of $\mathcal{S}_j$.
On the other hand, using Eqs. (2) and (3), first equation of system (1) derived at the ϵ^1 order reads:

$$\frac{\partial \psi}{\partial \tau_1} + \frac{1}{2}\left(i\sigma\omega_0 + c\right)\psi + \frac{1}{2}\left(\frac{ir}{\omega_0} - c_1\right)\varphi_1 + \frac{if}{2} = 0 \tag{11}$$

Including information of the SIM and defining $\Delta_1 = \delta_1 - \delta$, Eq. (11) becomes:

$$\begin{aligned} &\frac{\partial \psi}{\partial \tau_1} + \left(\frac{i\sigma\omega_0}{2} + \frac{c}{2}\right)\psi + \left(\frac{ir}{2\omega_0} - \frac{c_1}{2}\right)\phi_1 + \frac{if^0}{2} = 0 \\ \Leftrightarrow &\begin{cases} \dfrac{\partial N}{\partial \tau_1} = -\dfrac{c}{2}N + \left(\dfrac{r}{2\omega_0}\sin(\Delta_1) + \dfrac{c_1}{2}\cos(\Delta_1)\right)N_1 - \dfrac{f^0}{2}\sin(\delta) \\ \dfrac{\partial \delta}{\partial \tau_1} = -\dfrac{\sigma\omega_0}{2} - \left(\dfrac{r}{2\omega_0}\cos(\Delta_1) - \dfrac{c_1}{2}\sin(\Delta_1)\right)\dfrac{N_1}{N} - \dfrac{f^0}{2N}\cos(\delta) \end{cases} \end{aligned} \tag{12}$$

Injecting Eq. (12) into Eq. (10), a system of N_m equations is obtained, describing the behavior of the system at τ_1 time scale around the SIM:

$$\det(\mathbf{S})\mathbf{Id}_{N_m} \begin{pmatrix} \dfrac{\partial N_1}{\partial \tau_1} \\ \vdots \\ \dfrac{\partial N_{N_m}}{\partial \tau_1} \\ \dfrac{\partial \delta_1}{\partial \tau_1} \\ \vdots \\ \dfrac{\partial \delta_{N_m}}{\partial \tau_1} \end{pmatrix} = \underbrace{\begin{pmatrix} \mathcal{T}_1 \\ \vdots \\ \mathcal{T}_{N_m} \end{pmatrix}}_{\mathcal{T}} \tag{13}$$

where $\mathbf{Id}_{N_m}$ is the $N_m \times N_m$ unit matrix. This system is a reduced-order model of the asymptotic dynamics of the system. Indeed, using the SIM (Eq. (5)), one can express $\mathbf{S}$ and $\mathcal{T}$ as functions of two variables N_k and δ_l where k and l can be arbitrarily chosen.
Equilibrium points verify:

$$\begin{cases} \mathcal{T} = 0 \\ \det(\mathbf{S}) \neq 0 \end{cases} \tag{14}$$

Singular points verify:

$$\begin{cases} \mathcal{T} = 0 \\ \det(\mathbf{S}) = 0 \end{cases} \tag{15}$$

Examples of numerical simulations

All numerical results are obtained via direct integration of system equations (1). A Runge-Kutta scheme is used via the *ode45* function of Matlab. A 41-dof system ($N_m = 40$) is studied in this section using the following parameters: $\epsilon = 0.001$, $\omega_0 = 1$, $r = 3$, $c = 0.2$, $B = 2$, $c_1 = 2.8$ and $D = 50$. Initial conditions are $v(0) = 50$ and $\dot{v}(0) = \dot{u}_j(0) = u_j(0) = 0\ \forall j$.
For the first example, forcing parameters are the following: $f^0 = 35$ and $\sigma = 0$ (exact resonance of the main system). The projection of the SIM on the plane (N_{40}, N) is depicted in Fig. 2(a), where unstable zones are traced in red. Besides, the system possesses three stable equilibrium points, namely points no. 1, 2 and 3, and two singular points represented by black crosses. After being rapidly attracted by the SIM, the system could then, depending on initial conditions, tend to a periodic regime defined by one of the equilibrium points or face SMR around the first unstable zone. Figure 2(b) shows that the system behavior tends to a periodic regime as N (and all other phases and magnitudes) tends to a constant value. Comparison between the amplitudes of each oscillator predicted by equilibrium point no. 1 and final numeric amplitudes in Fig. 2(c) shows a good agreement. Finally, Fig. 2(d) depicts the modal behavior observed from numerical simulations during steady state.
In the second example, $f^0 = 170$ and $\sigma = 5$, the system has one unstable equilibrium point and six singular points (see Fig. 3(a)). Figures 3(b)-(c) show that the system faces SMR as expected and undergo repeated bifurcations between two modal behaviors, corresponding respectively to the behavior of the system around the lower and upper stable branches of the SIM encasing the second unstable zone. Indeed, it can be seen that the low amplitude modal behavior is the one observed in the first example.

Conclusion

Time multi-level energy exchanges and nonlinear interactions between a main forced linear system and a chain of nonlinear oscillators are studied. Detection of the slow invariant manifold and equilibrium and singular points at slow time scale enable to predict the behavior of the system. Those predictions are confronted to numerical results stemming from direct time integration of system equations, showing a good agreement. The analytical method presented provides design tools for tuning parameters of the chain in order to use it as a passive controller of the linear structure and/or for purposes of energy harvesting.

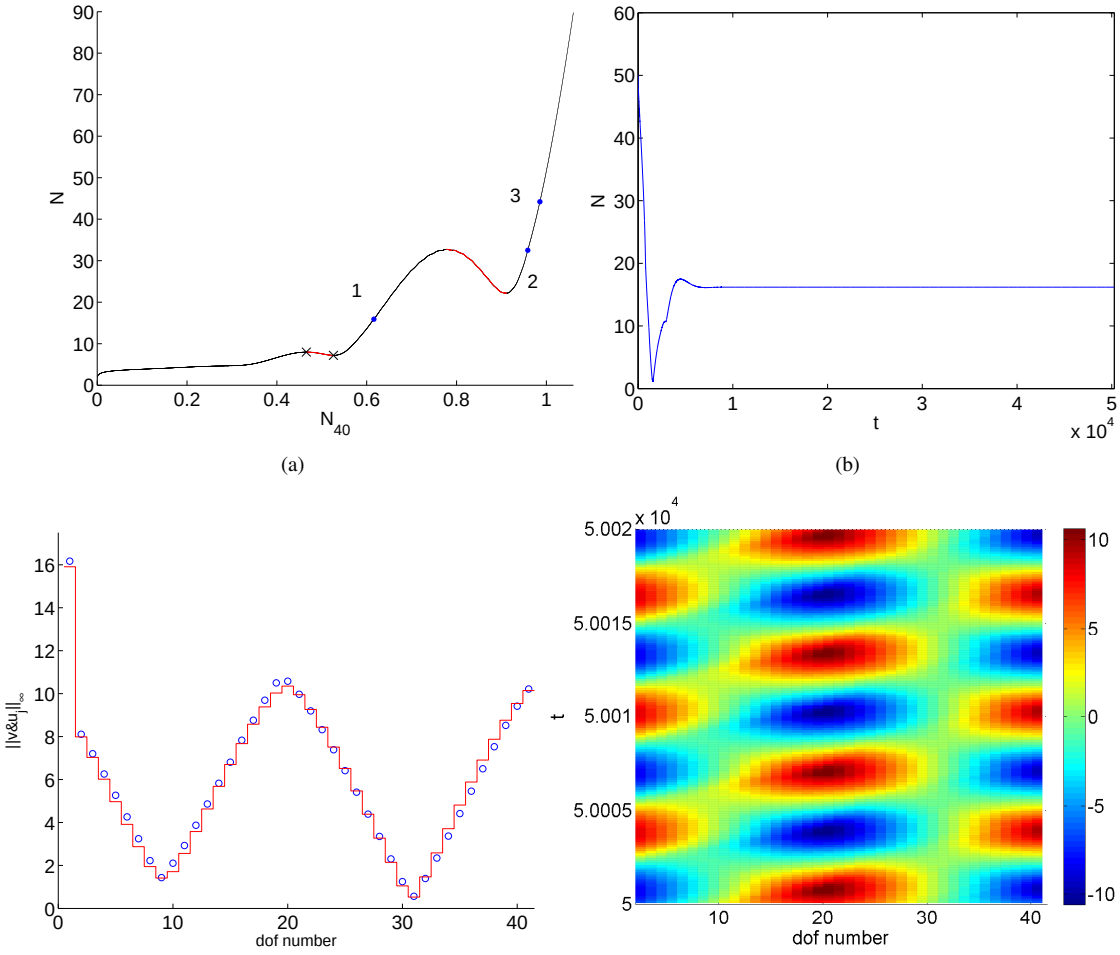

Figure 2: $N_m = 40$, $\epsilon = 0.001$, $\omega_0 = 1$, $r = 3$, $c = 0.2$, $B = 2$, $c_1 = 2.8$, $D = 50$, $\sigma = 0$ and $f^0 = 35$ - (a) SIM of the system (unstable zones are plotted in red). The system possesses three equilibrium points (no. 1, 2 and 3) and two singular points (black crosses), (b) N vs. time, (c) Comparison between system amplitudes obtained from analytical predictions corresponding to equilibrium point no. 1 (red lines) and numerical results at τ_1 time scale with all harmonics (blue circles), (d) Evolution of the amplitudes of oscillation of each mass of the chain obtained from numerical results at τ_1 time scale

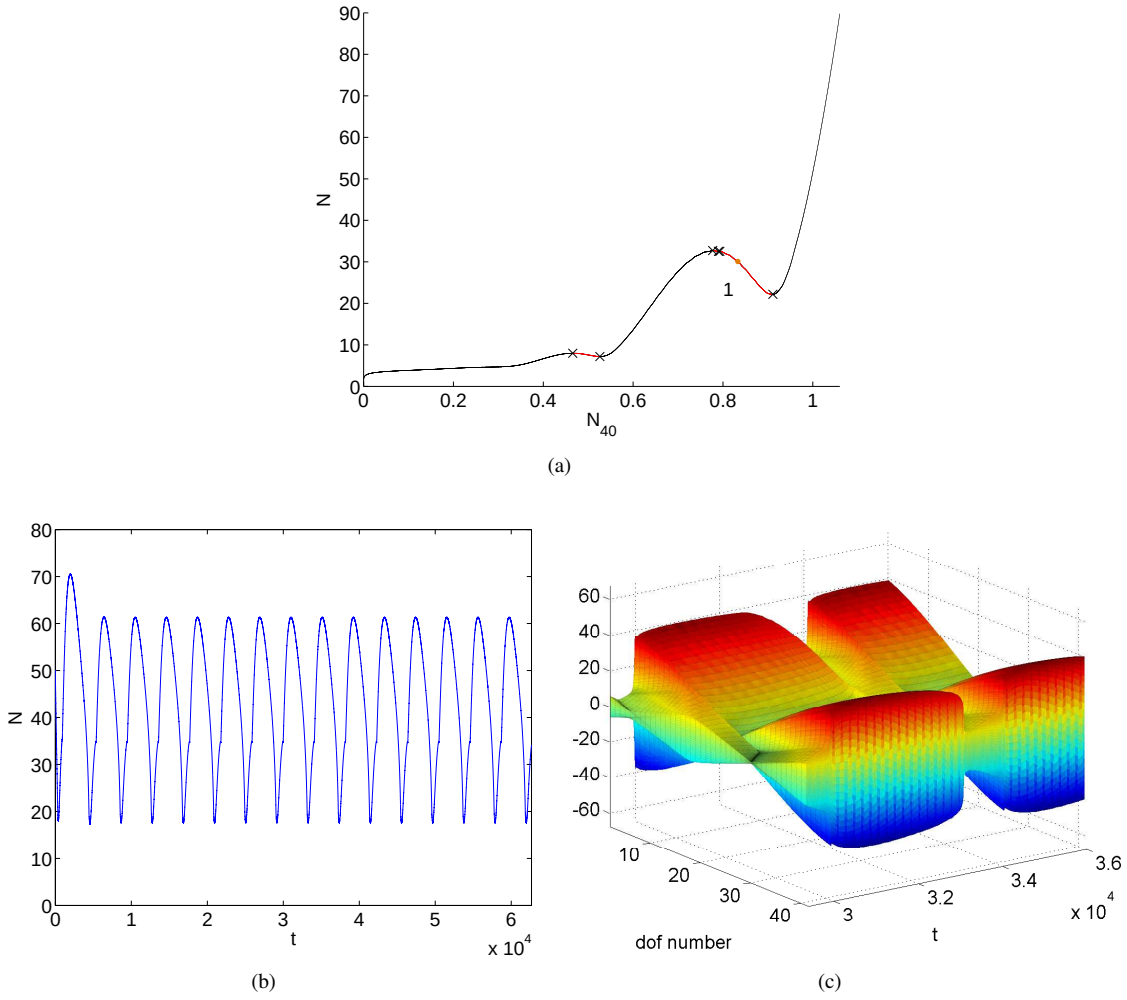

Figure 3: $N_m = 40$, $\epsilon = 0.001$, $\omega_0 = 1$, $r = 3$, $c = 0.2$, $B = 2$, $c_1 = 2.8$, $D = 50$, $\sigma = 5$ and $f^0 = 170$ - (a) SIM of the system (unstable zones are plotted in red). The system possesses one unstable equilibrium points (no. 1) and six singular points (black crosses), (b) N vs. time, (c) Evolution of the amplitudes of oscillation of each mass of the chain obtained from numerical results during SMR

References

[1] Roberson R. E. (1952) Synthesis of a nonlinear dynamic vibration absorber. *J. Frankl. Inst.* **254**:205–220

[2] Vakakis A. F., Gendelman O. V., Bergman L. A., McFarland D. M., Kerschen G. , Lee Y. S. (2009) Nonlinear Targeted Energy Transfer in Mechanical and Structural Systems, Springer, Netherlands.

[3] Gendelman O. V., Manevitch L. I., Vakakis A. F., M'Closkey R. (2000) Energy pumping in nonlinear mechanical oscillators: part I- dynamics of the underlying hamiltonian systems. *J. Appl. Mech.* **68**:34–41

[4] Vakakis A. F., Gendelman O. V. (2000) Energy pumping in nonlinear mechanical oscillators: part II - resonance capture. *J. Appl. Mech.* **68**:42–48

[5] Wierschem N., Luo J., Al-Shudeifat M., Hubbard S., Ott R., Fahnestock L., Quinn D., McFarland D., Spencer Jr. B., Vakakis A., Bergman L. (2014) Experimental testing and numerical simulation of a six-story structure incorporating two-degree-of-freedom nonlinear energy sink. *J. Struct. Eng.* **140**:04014027

[6] Tsakirtzis S., Kerschen G., Panagopoulos P. N., Vakakis A. F. (2005) Multi-frequency nonlinear energy transfer from linear oscillators to mdof essentially nonlinear attachments. *J. Sound Vib.* **285**:483–490

[7] Tsakirtzis S., Panagopoulos P. N., Kerschen G., Gendelman O. V., Vakakis A. F. , Bergman L. A. (2007) Complex dynamics and targeted energy transfer in linear oscillators coupled to multi-degree-of-freedom essentially nonlinear attachments. *Nonlin. Dyn.* **48**:285–318

[8] Starosvetsky Y., Vakakis A. F. (2011) Primary wave transmission in systems of elastic rods with granular interfaces. *Wave Motion* **48**:568–585

[9] Jayaprakash K. R., Vakakis A. F., Starosvetsky Y. (2013) Strongly nonlinear traveling waves in granular dimer chainss. *Mech. Syst. Signal Pr.* **39**:91–107

[10] Hasan M. A., Vakakis A. F., McFarland D. M. (2016) Nonlinear localization, passive wave arrest and traveling breathers in two-dimensional granular networks with discontinuous lateral boundary conditions. *Wave Motion* **60**:196–219.

[11] Ture Savadkoohi A., Lamarque C.-H., Weiss M., Vaurigaud B., Charlemagne S. (2016) Analysis of the 1:1 resonant energy exchanges between coupled oscillators with rheologies. *Nonlin. Dyn.* **86**:2145–2159.

[12] Manevitch L. I. (2001) The description of localized normal modes in a chain of nonlinear coupled oscillators using complex variables. *Nonlin. Dyn.* **25**:95–109.

[13] Nayfeh A. H., Mook D. T. (1979) Nonlinear Oscillations. John Wiley and Sons, NY.

[14] Starosvetsky Y., Gendelman O. V. (2008) Strongly modulated response in forced 2DOF oscillatory system with essential mass and potential asymmetry. *Physica D* **237**:1719–1733.